

Sea surface temperature and terrestrial biomarker records of the last 260 ka of core MD05-2904 from the northern South China Sea

HE Juan[†], ZHAO MeiXun, LI Li, WANG PinXian & GE HuangMin

State Key Laboratory of Marine Geology, Tongji University, Shanghai 200092, China

This paper reports high-resolution biomarker records of the last 260 ka for core MD05-2904 from the northern South China Sea (SCS). The sea surface temperature (SST) record using the $U_{37}^{k'}$ index reveals a minimum of 21.5°C (MIS 2) and a maximum of 28.3°C (MIS 5.5), for a temperature difference of almost 7°C, and provides the longest high-resolution $U_{37}^{k'}$ SST record in northern SCS. The content of odd-number long chain n -alkanes and several n -alkanes indexes such as the CPI, ACL and the C_{31}/C_{27} ratio, all reveal generally higher values during the glacials and lower values during the interglacials. Terrestrial input as indicated by n -alkane content was mostly controlled by sea-level changes: During the glacials, lower sea-level exposed the continental shelf to enable rivers to transport more terrestrial materials to the slope; and the situation reverses during the interglacials. The n -alkane indexes changes reveal more n -alkanes from contemporary vegetation during glacials as a result of the proximity of the core site to the source region, while the increases in ACL and C_{31}/C_{27} ratio during glacials indicate a change to more grassy vegetation. However, the highest values for CPI, ACL and the C_{31}/C_{27} ratio all occurred during late MIS 3, and it was suggested that this period was characterized by a strong summer monsoon-dominated humid climate which resulted in a denser vegetation for the exposed continental shelf region.

northern South China Sea, sea surface temperature, terrestrial input, source region vegetation

The South China Sea (SCS) is the largest marginal sea in the West Pacific, with wide continental shelf and significant river discharge. It has become a research focus of western Pacific paleoceanography due to the variety of marine and terrestrial environmental records preserved in its sediments, which yielded excellent results in deep-sea marine stratigraphy, paleoenvironmental changes, abrupt climate events and long-term changes in the ocean carbon reservoir. Many of paleoclimate and paleoceanography events revealed in the SCS sediments can be correlated to regional events and thus they have global significance. Biomarkers have been widely used for paleoceanographic and paleoenvironmental reconstruction, but their application has been limited in the SCS. Among the biomarkers, the $U_{37}^{k'}$ SST index based

on the ratio of alkenones has been successfully applied in the SCS. So far, long and high-resolution SST records have been generated for the south western SCS, but most records from the northern SCS are either short or low resolution^[1], so no millennial scale climate SST events were revealed. The long-chain n -alkanes (referred to as n -alkanes) produced by high land plants are carried to the marine sediments by river discharge or dusts, and they have been widely used in terrestrial environmental and vegetation reconstruction, but their application in

Received January 14, 2008; accepted May 12, 2008

doi: 10.1007/s11434-008-0289-2

[†]Corresponding author (email: crystalhejuan@163.com)

Supported by the National Natural Science Foundation of China (Grant Nos. 40676032, 40776029 and 40403012) and the Innovation Research Group of the National Natural Science Foundation of China (Grant No. 40621063)

the SCS has been few. Pelejero reported *n*-alkane content in the SCS and concluded that the *n*-alkane content was mostly, controlled by sea-level changes as increased terrestrial input during glacials also brought more *n*-alkanes^[2]. In addition, he also concluded that the source region vegetation type did not change significantly during glacial-interglacial cycles. Hu et al. reported similar results for core 17962 in the southern SCS, and they further concluded that the vegetation was mostly C_3 plant based on carbon isotope analysis^[3]. These results are in agreement with pollen records, indicating that aridity did not increase on the Sunda shelf during the last glacial^[4,5]. Climate and vegetation of the northern SCS, which have probably experienced more significant changes^[6], however, their effect on the *n*-alkane compose and isotope changes has not been thoroughly investigated.

The purpose of this paper is to report biomarker results for core MD05-2904 drilled from the northern slope of the SCS, and to discuss their paleoenvironment and paleo-vegetation implications. The $U_{37}^{k'}$ index is used to estimate the millennial scale SST changes for the last 260 ka, while the *n*-alkane content and various indexes are utilized to indicate the terrestrial environment and vegetation in this work, and comparison of these proxies is employed to reveal the relationship between the SCS SST and terrestrial climate change.

1 Materials and method

Core MD05-2904 (19°27.32'N, 116°15.15'E, 2066 m water depth) was recovered in 2005 during the “Marco Polo” cruise (Figure 1), as a collaboration project between China and France. The core is 44.98 m with quite uniform lithology consisting mostly of green-grey silt/clay with some sands. There are some slight bioturbations at a few places, and occasionally some sulfides, and some ashes at 543 cm^[7].

Our sampling resolution is every 8 cm for a total of 562 samples. The following biomarkers were analyzed: long-chain *n*-alkanes, long-chain alkanols, alkenones and sterols. The freeze-dried samples were manually ground, and after adding internal standards of *n*-C₂₄D₅₀, *n*-C₁₉H₃₉OH, about 2 g of samples was extracted by dichloromethane/methanol (3:1, V/V) ultrasonically. The supernatants were concentrated and then saponified with 6% KOH/methanol at room temperature overnight. Neutral components were extracted with *n*-hexane and

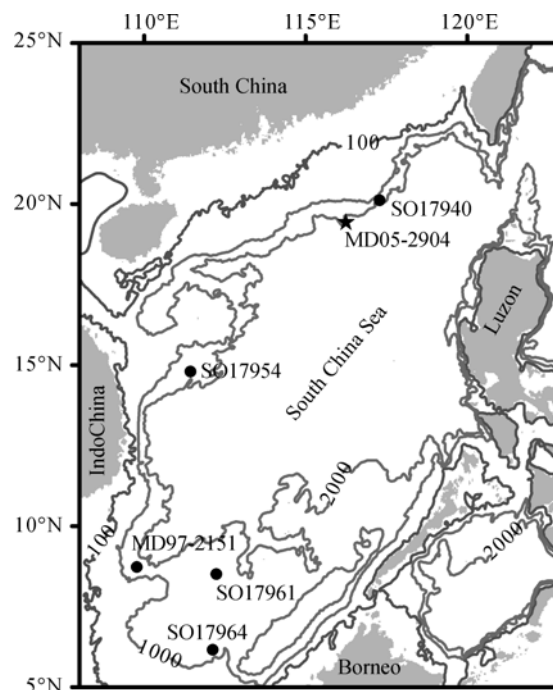


Figure 1 Location of core MD05-2904 (19°27.32'N, 116°15.15'E) and other core locations mentioned in the text. Bathymetry contours are indicated by dash lines.

then were further separated into two sub-fractions by silica gel column: hydrocarbons were eluted with *n*-hexane and the fraction containing *n*-alcohols, sterols and alkenones was eluted with dichloromethane/methanol (95:5, V/V). The hydrocarbon fraction was analysed directly using a gas chromatograph (GC), and second fraction was derived with N, O-bis(trimethylsilyl)-trifluoroacetamide (BSTFA) before GC analysis, with the following GC conditions: a HP-1 capillary column (60 m×0.32 mm×0.17 mm), the injector and FID detector both at 280°C, splitless injection, Helium as the carrier gas with a flow rate of 1.0 mL/min. Selected samples were examined by GC-MS for compound identification. Quantification of biomarkers was performed by integration of the relevant peak areas of biomarkers of interest and compared with those of the internal standards. All analyses were performed at the State Key Laboratory of Marine Geology of Tongji University. This paper reports the results of $U_{37}^{k'}$ SST, *n*-alkane content and other alkane indexes.

The age model for this core is established by correlating the planktonic foraminiferal (*G. ruber*) $\delta^{18}O$ curve of this core with the SPECMAP $\delta^{18}O$ curve and nearby core ODP 1144^[8] $\delta^{18}O$ curve. According to this model, the core bottom age is 256 ka, and our resolution

averages 0.5 ka.

2 Results and discussion

2.1 Sea surface temperature

The SST is calculated using the SCS calibration equation^[9]:

$$\text{SST } (^{\circ}\text{C}) = (U_{37}^{k'} - 0.092) / 0.031. \quad (1)$$

This SST record for the last 260 ka (extending to late MIS 8) reveals obvious glacial-interglacial cycles, and generally parallels the planktonic foraminiferal $\delta^{18}\text{O}$ record of this core (Figure 2A). The lowest SST is 21.5°C in MIS 2 and the highest is 28.3°C in MIS 5.5. SST fluctuated obviously during each Marine Isotope Stage (MIS), especially in substage of MIS 7 and 5. The SST for MIS 7.5 was 27.3°C while it was only 23.1°C for MIS 7.4, a difference of 4.2°C. The average SST for MIS 7.5 and 7.3 was both higher than that for the Holocene (25.5°C). However, SST for MIS 6 did not change significantly, with an average of 24.0°C, about 1°C

higher than that of MIS 2. SST for MIS 5 also changed significantly and the substages were clearly revealed. The SST for MIS 5.5 was 28.3°C, the highest for the last 260 ka. SST for MIS 5.2 was only 23.9°C, resulting in SST range of 4.4°C for MIS 5. MIS 5.5 SST was 1.6°C higher than that of the Holocene, and MIS 5.2 SST was similar to that of MIS 6 average. The average SST for MIS 4 was 23.7°C, that for MIS 3 was 23.5°C and characterized by frequent but small oscillations. MIS 2 SST was the lowest during the last 260 ka with frequent and large oscillations. The lowest SST (21.5°C) was recorded at 15.5 ka, increased to 24.5°C during the Bølling-Allerød event, followed by a sudden decrease to 23.6°C during the Younger Dryas, and gradual increase to ca. 26°C during the Holocene. The coretop $U_{37}^{k'}$ SST is similar to the modern annual SST for the site, supporting to applicability of the $U_{37}^{k'}$ index for the SCS.

Both the absolute values and the general trend revealed by our MD05-2904 SST record are similar to

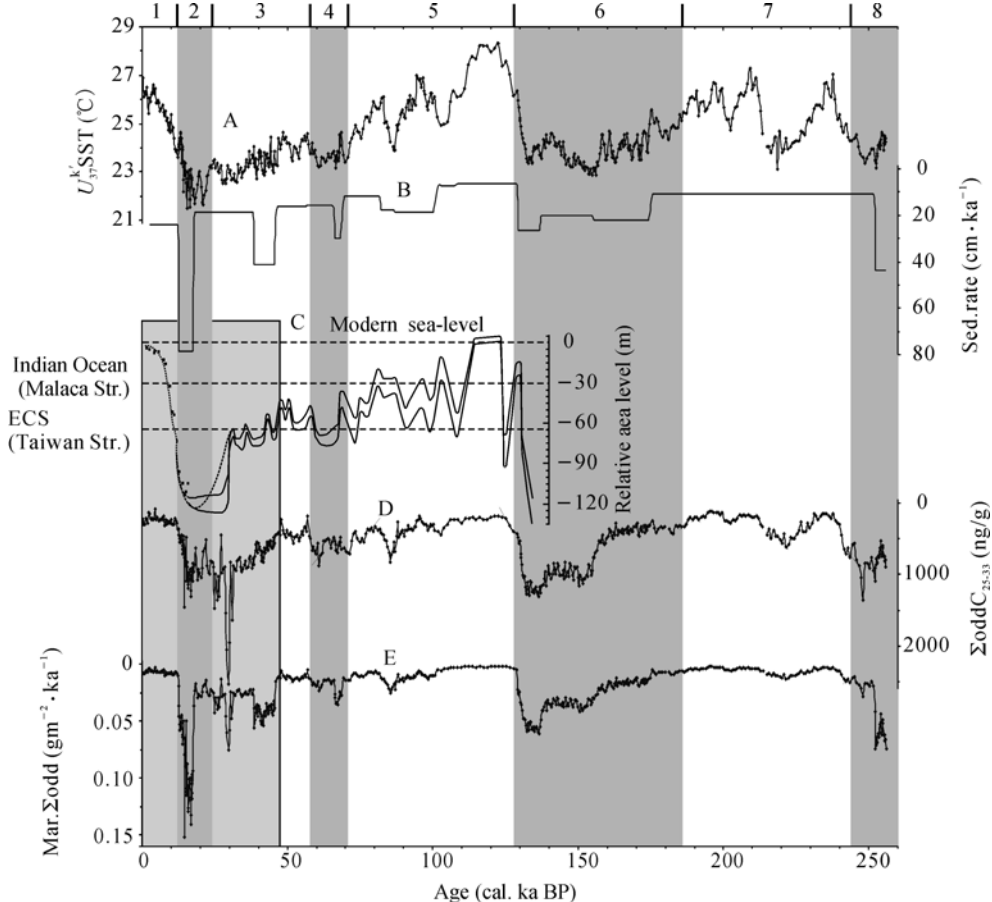


Figure 2 Proxy records for core MD05-2904: SST (A), bulk sedimentation (B), sea-level curve (C) from ref. [15], the content (D) and MAR (E) of long-chain odd-carbon number alkanes. The shaded vertical bars indicate intervals of sea level lower than -65 m.

previous reports, but this record provides the longest high-resolution record to afford detailed discussion of SST changes for the last three glacial-interglacial cycles. For example, among the three terminations, the SST change was only 3.3°C from MIS 8 to MIS 7, smaller than changes for the MIS 6 to MIS 5 (4.9°C) and the MIS 2 to MIS 1 (4.3°C) transitions. SST changes for substages of MIS 7 and MIS 5 were clearly revealed with amplitudes of 2–3°C. For the three glacials, the SST for MIS 8 and MIS 6 was around 24°C, higher than that for MIS 2 (23°C). For the three interglacials, the SST for MIS 7 and MIS 1 was around 25.4°C, lower than that for MIS 5 (25.8°C). The trend for MIS 5 is very similar to that revealed by the MD 97-2151 SST record from the southwestern SCS^[10]. Millennial scale SST changes were also different for different MIS stages, for example, they were obvious for the late MIS 7 and for the MIS 7 to MIS 6 transition. For MIS 4 and MIS 3, such SST changes were also conspicuous and some oscillations were similar to the millennial scale changes recorded in the Greenland icecore. The record also clearly registered the YD and B/A event during the last termination.

2.2 *n*-alkanes and terrestrial input

In general, *n*-alkanes from high land plant waxes have carbon numbers ranging from C₂₁ to C₃₅, with the C₂₉, C₃₁ or C₃₃ as the most abundant. They also have a clear odd-carbon number dominance^[11,12]. The *n*-alkanes produced by algae range from C₁₁ to C₂₅, with C₁₇ or C₁₉ as the most abundant and without an odd-even carbon dominance^[12].

For core MD05-2904, the *n*-alkanes range from C₁₂ to C₃₅, but most are from C₁₇ to C₃₃, and C₂₉ or C₃₁ *n*-alkane is the most abundant in almost all samples. The total content of odd C₂₅ to C₃₃ *n*-alkanes is refereed as the total *n*-alkane content and is used as a proxy for terrestrial input, which is transported by river discharge or dust. The total *n*-alkane content ranges from 91 to 2491 ng/g, with a clear glacial-interglacial oscillation pattern (Figure 2D).

With a few exceptions, the maximum values for the three glacials (MIS 8, 6 and 2) were within 1000–1300 ng/g. The values for MIS 4 were also higher, but they were much lower than those for MIS 8, 6 and 2. For the three interglacials, the minimum values were similar at ca. 200 ng/g, but the values for the Holocene were lower

(91 ng/g). For the warmer intervals of MIS 7 and MIS 5, the total *n*-alkane content was slightly higher. One marked feature is that the highest values during the last 260 ka were recorded during late MIS 3. Generally speaking, total *n*-alkane and SST are inversely correlated with a relatively good linear relationship ($R^2 = 0.46$).

To take into account of the sedimentation rate effect (Figure 2B), *n*-alkane mass accumulation rate (MAR) is calculated (Figure 2E) and compared with *n*-alkane content (Figure 2D). The *n*-alkane MAR is calculated by the following Chen et al.'s^[13] equation:

$$\text{MAR} \Sigma \text{ odd} = \text{SR} \times (\text{BD} - P \times \text{WD}) \times \text{wt}\%, \quad (2)$$

where *SR* is the linear sedimentation rate (cm/ka); *BD* is wet bulk density (g/cm³), measured on board by the multisensor track; *WD* is seawater density (1.025 g/cm³); wt% is total *n*-alkane content; *P* is porosity, calculated by $P = 0.7263 \times e^{-z/1064}$ ^[14], where *z* is the sediment depth.

The *n*-alkane MAR curve reveals an even clearer trend of higher glacial values and lower interglacial values (Figure 2E). The highest values occurred in MIS 2, but two intervals in MIS 3 also had higher values which were similar to the MIS 6 values. Both *n*-alkane content and MAR records show smaller changes in MIS 7 and 5, in contrast to the marked SST changes. This comparison suggests that *n*-alkane content was not controlled by SST. Our record is in agreement with previous result, providing farther evidence that *n*-alkane content in the SCS sediment was mostly controlled by sea-level changes which in turn influenced terrestrial input^[2]. During the glacials, lower sea level exposed the continental shelf, extended the coastal line to the outer shelf region and increased terrestrial input to the core site. During the last glacial maximum, when sea level was lower by 100–120 m, corresponding approximately to the present 100 m contour region (Figure 1), the alkane content and MAR both showed high values. The sea-level variation since MIS 6 is displayed in Figure 2C. It can be seen from the curves that sea level had some effect on *n*-alkane content, for example, the major *n*-alkane variations during MIS 3 and 2 all correlated to sea-level drops. Moreover, drier climate and stronger winter monsoon during the glacials likely increased dust input to the SCS and brought more *n*-alkanes to the SCS. During the interglacials, rising sea-level flooded the continental shelf, river mouth retreated, terrestrial input to the continental slope region decreased. In addition, dust input also decreased, all contributed to lower

n-alkane content in the SCS. The higher *n*-alkane content in late MIS 3 was most likely related to summer monsoon strength. Lake records from the Tibetan Plateau, sediment records from the northern SCS all reveal that precipitation was higher during MIS 3 [16,17]. Pollen record and factor analysis for core SO17940 showed that source region humidity increased significantly during MIS 3 [17]. The record of coarser charcoal also had its peak values during MIS 3 [18], which was interpreted to reflect higher humidity and rainfall that brought the originally deposited charcoal to the site. As for the *n*-alkane, wet climate increased terrestrial vegetation growth and density, which produced more *n*-alkanes to be transported to the site. This result suggests that sedimentary *n*-alkane content is not solely controlled by sea level, it also relates to the source region climate and vegetation density.

The best environmental condition for *n*-alkane transport to marine sediment is humid climate during low sea-level stand. Humid climate favors vegetation growth to produce large amounts of *n*-alkanes, and lower sea level favors the transportation of *n*-alkanes to the shelf and slope regions. Our interpretation of the MIS 3 *n*-alkane result needs verification by multi-proxy research, especially the analysis of carbon and hydrogen isotopes, both are related to precipitation and vegetation types (C₃ vs. C₄).

2.3 *n*-alkane indexes and source region vegetation and climate

Several indexes based on *n*-alkane compositions have been used to estimate the sources of these *n*-alkanes and to reconstruct source region vegetation type and climate. They include CPI, ACL and A.I., and their definitions

and proxy information are listed in Table 1. As discussed above, high land plants *n*-alkanes have strong odd over even carbon preference, and this preference decreases with degradation and diagenesis. Therefore, CPI can be used to indicate *n*-alkane source and maturation. ACL and A.I. are established based on the observation that the most abundant *n*-alkanes have different carbon number in different vegetations. For example, although both grass and trees produce C₂₇, C₂₉ and C₃₁ *n*-alkanes, C₃₁ *n*-alkane is often the most abundant in grass while C₂₇ or C₂₉ *n*-alkane is usually the most abundant in trees. Thus, ACL and A.I. can be used to reflect vegetation types, with increasing values indicating more grass contribution [19,20].

The CPI values of the core range from 1.2 to 5.1, and most are higher than 2 (Figure 3C), indicating that the *n*-alkanes were mostly from contemporary vegetation. ACL has a range of 28.7 to 30.1 (Figure 3D) with an average value of 29.3. Overall, CPI and ACL have similar glacial-interglacial variations over the last 260 ka, with lower values during interglacial intervals of MIS 7.5, 7.3, 5.5, 5.3, 5.1, early MIS 3 and the Holocene, and higher values during glacial intervals of MIS 8, 7.4, 6, 5.2, 4, late MIS 3 and 2. However, CPI and ACL have almost no linear relationship with SST ($R^2_{CPI}=0.09$, $R^2_{ACL}=0.07$), partially due to the fact that their variations are not synchronous. In addition, although lower CPI and ACL values occurred during warm intervals, the values do not have quantitative relationships. For example, MIS 5.5 SST is 1.6°C higher than Holocene SST, but the MIS 5.5 CPI is 1.5 units higher than the Holocene value. MIS 3 SST is not very low, but the corresponding CPI and ACL values are the highest during the

Table 1 *n*-alkane indexes and their proxy implication

Index	Equation	Proxy implication
$\Sigma \text{Odd}(C_{25-33})$	$\Sigma \text{Odd}(C_{25-33})=C_{25}+C_{27}+C_{29}+C_{31}+C_{33}$	Terrestrial (high plant) input, controlled by sea level
CPI (Carbon Preference Index)	$CPI = \frac{1}{2} \left[\frac{\sum C_{25} - C_{33} (\text{odd})}{\sum C_{24} - C_{32} (\text{even})} + \frac{\sum C_{25} - C_{33} (\text{odd})}{\sum C_{26} - C_{34} (\text{even})} \right]$	Maturation index to distinguish fresh vegetation alkane or fossil alkane. Fresh land vegetation <i>n</i> -alkane CPI > 3
ACL (Average Chain Length)	$ACL = \frac{[C_{25}] \times 25 + [C_{27}] \times 27 + [C_{29}] \times 29 + [C_{31}] \times 31 + [C_{33}] \times 33}{[C_{25}] + [C_{27}] + [C_{29}] + [C_{31}] + [C_{33}]}$	Vegetation type index. Higher for grass vegetation, lower for trees
A.I. (Alkane Index)	$A.I. = C_{31} / (C_{31} + C_{29})$	Vegetation type index. Higher for grass vegetation, lower for trees
C_{31}/C_{27}	C_{31}/C_{27}	Vegetation type index. Higher for grass vegetation, lower for trees

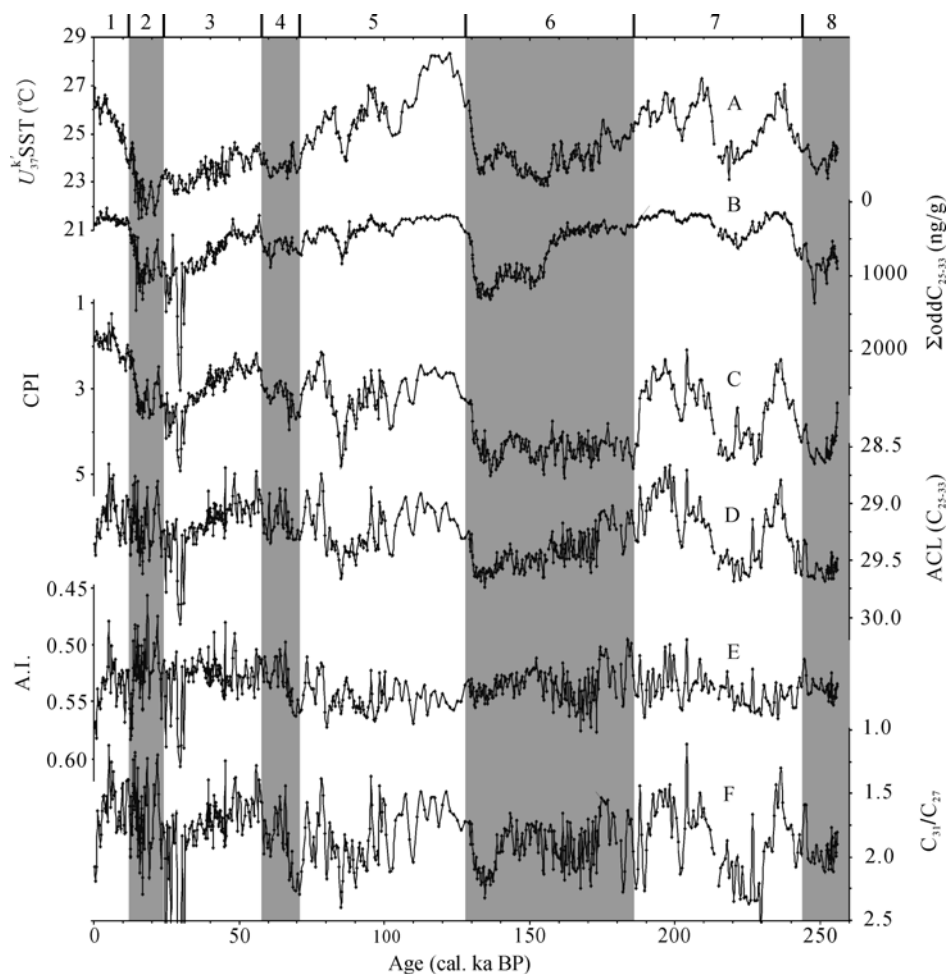


Figure 3 SST and *n*-alkane indexes for MD05-2904. A, SST; B, the content of long-chain odd-carbon number alkanes (C_{25} - C_{33}); C, CPI (Carbon Preference Index); D, ACL (Average Chain Length); E, A.I. (Alkane Index); F, C_{31}/C_{27} .

last 260 ka. These factors suggest that CPI, ACL and SST can only be compared for their general trends, there are no quantitative relationships.

Previous research has suggested higher source region temperature would result in higher ACL [21,22], but our results reveal higher ACL during glacial. Thus, the ACL variations could not be controlled by temperature, instead they reflect mainly source region vegetation changes. Higher values during the glacial suggest increased grass vegetation, in agreement with published pollen records [6,23–25]. CPI and ACL have some correlations with total *n*-alkane content ($R_{\text{CPI}}^2=0.22$, $R_{\text{ACL}}^2=0.36$), with higher values during glacial for all three parameters, for example, during late MIS 8, late MIS 6, and early MIS 2. These relationships suggest that increased *n*-alkanes also mean they are more characteristic of contemporary land plant *n*-alkanes. One explanation is that dense vegetation occurred on exposed shelf during the glacial to produce *n*-alkanes, and they were

quickly transported to the slope to result in higher CPI. The higher grass contribution would also increase ACL. On the contrary, *n*-alkane content, CPI and ACL were all lower during the interglacials (especially the Holocene), indicating that the *n*-alkanes lack the characteristics of contemporary vegetations and a significant portion was from diagenetic altered plant *n*-alkanes. Furthermore, lower ACL values suggest that grass contribution was also lower during the interglacials. An alternate explanation could be that dust transportation of terrestrial materials to the SCS increased during the glacial, and dusts probably transported mostly contemporary *n*-alkanes from vegetation and surface soils, resulting in higher CPI and ACL. During interglacials, river input would increase, which could carry fossil *n*-alkanes with lower CPI and ACL. Both the *n*-alkane content and CPI reached maximum values in late MIS 3, probably due to the transportation of contemporary *n*-alkanes produced by the dense vegetation. This inference is in agreement

with the conclusion reached in the last section, which suggested that the higher ACL values were a result of increased grass vegetation under humid climate in late MIS 3. Again, this inference needs to be verified by carbon and hydrogen isotope measurements of *n*-alkanes, as the former can be used to distinguish C₃ vs. C₄ vegetation and the latter can be used to reflect precipitation amount. Meanwhile, CPI and ACL variations could also be related to sudden sea-level changes. Maximum values corresponded to rapid sea-level drops, with some uncertainties of age models.

The variation of A.I. for core MD05-2904 did not show any particular pattern (Figure 3E), but the C₃₁/C₂₇ ratio revealed a general trend of higher values in the glacials and lower values in the interglacials (Figure 3F). The C₃₁/C₂₇ ratio has no correlation with SST ($R^2 = 0.02$), some correlation with *n*-alkane content ($R^2 = 0.24$), but good correlation with CPI ($R^2 = 0.32$) and ACL ($R^2 = 0.63$). The C₃₁/C₂₇ ratio corroborates the conclusions based on CPI and ACL that grass vegetation increased during the glacials.

Published pollen records from the northern SCS slope showed that the dominant vegetation oscillated between herb and *Pinus* during glacial to interglacial cycles. It was suggested that during glacial times, under a relatively dry and cool climate, the exposed northern continental shelf due to the lowering of sea level was covered by grassland, mainly *Artemisia*, *Gramineae* and *Cyperaceae*. Pollen in these sediments was mainly from the exposed shelf, and the distance between source and core site was shortened. The study site could receive great amounts of herbaceous pollen during glacials even though they normally could not be dispersed far away. During interglacial times when sea level was higher, the continental shelf was submerged, pollen amount especially those herb pollen decreased. Most pollen were from the north, with the easily dispersed *Pinus* pollen predominant^[6,23–25]. The pollen diagram of SO17940 also displays sub-orbital variations in vegetation and climate, suggesting alternating predominance of relatively cool/humid and dry/temperate cycles on millennial scale during the glacial period^[25]. Our alkane index of CPI, ACL and C₃₁/C₂₇ ratio all reveal high values in the glacials and low values in the interglacials, reflecting changes in source vegetation that herbaceous plants increased in glacial times, and decreased in the interglacial times. Comparison of the biomarker and pollen records

shows that the general trends agree to some extent but the details differ. For example, the variation of herb/*Pinus* was small before MIS 5 in ODP 1144^[6], but the alkane index of herb/tree in our work varied greatly. And there are timing differences in alkane index and pollen record (including charcoal), so much as no corresponding^[6,18,23–27]. There are two possibilities for such discrepancies. First, the route and mechanism of transport are different. Just as mentioned above, pollen content in the ocean sediment is closely related with its source, the route and mechanism of pollen transport to the sea. For example, during the glacial, herbaceous pollen content was high due to their short distance to site. But at the same time, prevailing winter monsoon could also bring more *Pinus*'s, so herbs vs. pine diagram in sediments could not represent their ratio in vegetation. Sun and Luo^[6] believe the herbs vs. pine index in ODP1144 “closely related with the distance between source and study site”, in other words, “the eustatic sea level changes of the glacial cycles, and the extent of the continental shelf exposed”. In contrast, *n*-alkanes were mostly transported by rivers^[2], wind speed has little effect on their content in marine sediments. In addition, the transportation distance also has less influence on the alkane indexes (ACL, and C₃₁/C₂₇ ratio) than it does on pollen. Secondly, the uncertainties associated with the different dating methods and the different sampling resolution make the direct comparison between pollen and biomarkers different. The pollen record by Sun and Luo^[6] and charcoal record by Luo et al.^[26] were based on chronologies generated by biostratigraphy, resulting in a preliminary age with lower sampling resolution. Our records correlate better with the higher resolution pollen^[23–25] and charcoal^[18,27] records for ODP1144 and SO17940, for example all had higher values in late MIS3 and MIS2 with similar amplitude oscillations^[18,24,25]. But there are some differences, for example, there are three grass pollen peaks from ca. 36 ka to 24 ka in MIS3^[24], but our biomarker had higher values from ca. 31 ka to 24 ka, with the maximum at 30 ka. Grass pollen in ODP1144 increased from 28 ka, reached a maximum at 18 ka, followed by a gradual decrease^[24]. The alkane indexes oscillated between 22 ka and 17 ka, and reached a maximum at 17 ka, followed by decreases.

The increase in grass vegetation during the glacials was mostly a result of drier climate. But lower PCO₂

during the glaci-als also favored grass growth. Most grasses are C_4 plants which possess a “ CO_2 concentrating mechanism” to enable them to out-compete C_3 plants under lower CO_2 environment^[28,29]. However, the previously used grass/tree index of A.I. has no glacial-interglacial pattern in our core. Part of the reason is that there is no clear predominance pattern between C_{29} and C_{31} n -alkane among some important species of the region: *Artemisia*, *Pinus* and *Betula*^[30]. Thus, C_{27} n -alkane variation is a better proxy for the vegetation change surrounding the northern SCS, with the C_{31}/C_{27} ratio reflecting grass/tree ratios. The various n -alkane indexes also reveal many minor grass/tree oscillations during the glaci-als and interglaci-als. Such oscillations have also been recorded in pollen records from core SO17940 and in the Tianyang Lake record from Leizhou Peninsula^[31], but detailed comparison is not made here due to the large uncertainties of the different age models. Both ACL and the C_{31}/C_{27} ratio reveal the highest values during late MIS 3, suggesting that the continental climate was probably relatively warm and wet, favoring the growth of some grasses. Thus, the large increase in total n -alkane content was mainly due to the increase of these grasses. Again, these inferences need to be verified by carbon and hydrogen isotope analyses.

3 Conclusions

We have carried out high resolution organic geochemical analyses of core MD05-2904 from the northern SCS to obtain SST, terrestrial input and vegetation records for

the last 260 ka. The results are summarized below:

(1) The 260 ka SST record revealed a minimum of $21.5^\circ C$ (MIS 2), maximum of $28.3^\circ C$ (MIS 5.5) for a difference of near $7^\circ C$. The SST difference for both Terminations II and I are ca. $5^\circ C$, but it is only $3^\circ C$ for Termination III. The YD and B/A events were clearly revealed, but other millennial scale SST oscillations need further study with a better constrained age model.

(2) The total n -alkane content record has a clear pattern of higher values during the glaci-als and lower values during the interglaci-als, mostly controlled by sea-level changes.

(3) CPI has a general trend of higher values during the glaci-als and lower values during the interglaci-als, indicating that glacial n -alkanes were more characteristic of contemporary vegetation due to their approximate to the source region.

(4) ACL and C_{31}/C_{27} ratio also have a general trend of higher values during the glaci-als and lower values during the interglaci-als, suggesting more grass vegetation during the glaci-als.

(5) n -alkane content, CPI, ACL and the C_{31}/C_{27} ratio all reveal maximum values in late MIS 3, indicating a special environment. It is most likely that the humid climate supported dense vegetation, especially more grass vegetation under lower PCO_2 .

The samples used in this study were retrieved during the IMAGES XII, MD-147-Marco Polo Cruise of the R/V Marion Dufresne of the French Polar Institute (IPEV). We thank Prof. Sun Xiangjun for her constructive comments and suggestions on the manuscript and Wang Hui for her technical assistant.

- 1 Pelejero C, Grimalt J O, Heilig S, et al. High-resolution U_{37}^k temperature reconstructions in the South China Sea over the past 220 kyr. *Paleoceanography*, 1999, 14(2): 224–231[[doi](#)]
- 2 Pelejero C. Terrigenous n -alkane input in the South China Sea: high-resolution records and surface sediments. *Chem Geol*, 2003, 200: 89–103[[doi](#)]
- 3 Hu J F, Peng P A, Jia G D, et al. Biological markers and their carbon isotopes as an approach to the paleoenvironmental reconstruction of Nansha area, South China Sea, during the last 30 ka. *Org Geochem*, 2002, 33: 1197–1204[[doi](#)]
- 4 Sun X J, Li X, Luo Y L. Vegetation and climate on the Sunda Shelf of the South China Sea during the Last Glaciation-pollen results from station 17962. *Acta Bot Sin*, 2002, 44(6): 746–752
- 5 Li X, Sun X J. Palynological records since Last Glacial Maximum from a deep sea core in southern South China Sea. *Quat Sci (in Chinese)*, 1999, 6: 526–535
- 6 Sun X J, Luo Y L. Pollen record of the last 280 ka from deep-sea sediments of the northern South China Sea. *Sci China Ser D-Earth Sci (in Chinese)*, 2001, 31(10): 846–853
- 7 Laj C, Wang P X, Balut Y, et al. MD147-Marco Polo IMAGES XII Cruise Report. France: Institut Paul-Emile Victor (IPEV), 2005
- 8 Bühring C, Sarnthein M, Erlenkeuser H. Toward a high-resolution stable isotope stratigraphy of the last 1.1 m.y.: Site 1144, South China Sea. In: Prell W L, Wang P, Blum P, et al., eds. *Proceedings of the Ocean Drilling Program, Scientific Results, Vol. 184*. College Station Texas. 2004. 1–29
- 9 Pelejero C, Grimalt J O. The correlation between the U_{37}^k index and sea surface temperatures in the warm boundary: the South China Sea. *Geochim Cosmochim Acta*, 1997, 61(22): 4789–4797[[doi](#)]
- 10 Zhao M X, Huang C Y, Wang C C, et al. A millennial-scale U_{37}^k sea-surface temperature record from the South China Sea ($8^\circ N$) over the last 150 kyr: Monsoon and sea-level influence. *Palaeogeogr, Pa-*

- laeoclimatol, *Palaeoecol*, 2006, 236(2): 39–55[[doi](#)]
- 11 Eglinton G, Hamilton R J. Leaf epicuticular waxes. *Science*, 1967, 156: 1322–1335[[doi](#)]
 - 12 Meyers P A, Ishiwatari R. Lacustrine organic geochemistry- an overview of indicators of organic matter sources and diagenesis in lake sediments. *Org Geochem*, 1993, 20: 867–900[[doi](#)]
 - 13 Chen M T, Shiao L J, Yu P S, et al. 500000-Year records of carbonate, organic carbon, and foraminiferal sea-surface temperature from the southeastern South China Sea (near Palawan Island), *Palaeogeogr, Palaeoclimatol, Palaeoecol*, 2003, 197: 113–131[[doi](#)]
 - 14 Huang W, Wang P X. The Statistics of Sediment Mass in the South China Sea: Method and Result. *Adv Earth Sci (in Chinese)*, 2006, 21(5): 465–473
 - 15 Higginson M J, Maxwell J R, Altabet M A. Nitrogen isotope and chlorin paleoproductivity records from the Northern South China Sea: remote vs. local forcing of millennia- and orbital-scale variability. *Mar Geol*, 2003, 201: 223–250[[doi](#)]
 - 16 Shi Y F, Yu G, Liu X D, et al. Reconstruction of the 30–40 ka BP enhanced Indian monsoon climate based on geological records from the Tibetan Plateau. *Palaeogeogr, Palaeoclimatol, Palaeoecol*, 2001, 169: 69–83[[doi](#)]
 - 17 Luo Y L, Sun X J. Vegetation evolution in the northern South China Sea region since 40 ka BP— an attempt to reconstruct palaeovegetation based on biomization. *Acta Bot Sin*, 2001, 43(11): 1202–1206
 - 18 Sun X J, Li X, Chen H C. Evidence for natural fire and climate history since 37 ka BP in the northern part of the South China Sea. *China Sea. Sci China Ser D-Earth Sci*, 2000, 43(5): 487–493
 - 19 Maffei M. Chemotaxonomic significance of leaf wax alkanes in the Gramineae. *Biochem System Ecol*, 1996, 24: 53–64[[doi](#)]
 - 20 Zhang Z H, Zhao M X, Eglinton G, et al. Leaf wax lipids as paleovegetational and paleoenvironmental proxies for the Chinese Loess Plateau over the last 170 ka. *Quat Sci Rev*, 2006, 25: 575–594[[doi](#)]
 - 21 Hinrichs K U, Rinna J, Rullkoetter J. Late Quaternary paleoenvironmental conditions indicated by marine and terrestrial molecular biomarkers in sediments from the Santa Barbara Basin. In: Wilson R C, Tharp V L, eds. *Proceedings of the Fourteenth Annual Pacific Climate Workshop*. California Department of Water Resources, 1997. 1–9
 - 22 Kawamura K, Ishimura Y, Yamazaki K. Four years' observations of terrestrial lipid class compounds in marine aerosols from the western North Pacific. *Global Biogeochem Cycles*, 2003, 17[[doi](#)]
 - 23 Luo Y L, Sun X J. Vegetation evolution during the Last Penultimate Glacial Cycle: a high-resolution pollen record from ODP site 1144, the South China Sea. *Mar Geol Quat Geol (in Chinese)*, 2003, 23(1): 19–25
 - 24 Luo Y L, Sun X J. Vegetation evolution and millennial-scale climatic fluctuations since Last Glacial Maximum in pollen record from northern South China Sea. *Chin Sci Bull*, 2005, 50(8): 793–799
 - 25 Sun X J, Li X. A pollen record of the last 37 ka in deep sea core 17940 from the northern slope of the South China Sea. *Mar Geol*, 1999, 156: 227–244[[doi](#)]
 - 26 Luo Y L, Chen H C, Wu G X, et al. Records of natural fire and climate history during the last three glacial-interglacial cycles around the South China Sea—charcoal record from the ODP 1144, in South China Sea. *Sci China Ser D-Earth Sci*, 2001, 44(10): 897–904
 - 27 Luo Y L, Sun X J, Chen H C. Millions years record of natural fire and climate history in the northern South China Sea — charcoal record from the deep sea core ODP 1144. *Chin Sci Bul (in Chinese)*, 2006, 51(8): 942–950
 - 28 Cerling T E, Harris J M, MacFadden B J, et al. Global vegetation change through the Miocene/Pliocene boundary. *Nature*, 1997, 389: 153–158[[doi](#)]
 - 29 He J, Wang P X. Vegetation change in late Miocene and evolution of photosynthesis. *Adv Earth Sci*, 2005, 6: 618–626
 - 30 Schwark L, Zink K, Lechterbeck J. Reconstruction of postglacial to early Holocene vegetation history in terrestrial Central Europe via cuticular lipid biomarkers and pollen records from lake sediments. *Geology*, 2002, 30: 463–466 [[doi](#)]
 - 31 Zheng Z, Lei Z Q. A 400,000 year record of vegetational and climatic changes from a volcanic basin, Leizhou Peninsula, southern China. *Palaeogeogr, Palaeoclimatol, Palaeoecol*, 1999, 145: 339–362[[doi](#)]